MACHINE VISION IMPLEMENTATION FOR OFF-LINE MEASUREMENT OF WELD BEAD GEOMETRY IN API X65 PIPELINE STEEL

Mohammad Ali MORADPOUR[1] , Sayyed Hojjat HASHEMI[2], Khalil KHALILI[3]

In this paper, machine vision is used for measurement of weld bead geometry in submerged arc welding of API X65 steel plates. First, different welding parameters including voltage, current and speed are set to perform the SAW with different heat inputs. Then, different etchants are used to find an appropriate solution for the best revelation of weld metal in the cross section of welded plates. Finally, weld bead parameters (including weld width, depth, height, area and boundary) are measured using machine vision technology and image processing techniques. The comparison of machine vision results with those from manual measurements showed the higher accuracy of the proposed vision system and its faster performance in accurate measurement of weld bead geometry.

Keywords: API X65 steel; automated visual measurement; submerged arc welding; weld bead geometry.

1. Introduction

The submerged arc welding (SAW) is one of the critical stages in the manufacturing process of gas transmission pipes, because different defects could be developed in the weld seam during the welding process such as incomplete penetration, slag inclusions and etc. [1]. Thus, obtaining the desired welding quality is a basic goal in the manufacturing processes of such pipes. On the other hand, weld bead geometry directly affects the weld quality [2]. In fact, the desired weld bead geometry guarantees the preferred welding quality. As it is shown in Fig. 1, weld bead geometry includes different parameters such as depth of penetration (P), bead width (W) and height (H), bead convexity length (B_R), length of bead penetration boundary (B_P) and bead total area (weld metal area) which includes bead reinforcement area (A_R) and bead penetration area (A_P) [3]. Each weld parameter (especially the depth of penetration), has a key role in the final weld quality.

[1] MSc., Dept. of Mechanical Engineering, University of Birjand, Iran,
e-mail: moradpour.mamad@yahoo.com
[2] Prof., Dept. of Mechanical Engineering, University of Birjand, Iran,
e-mail: shhashemi@birjand.ac.ir
[3] Assoc. Prof., Dept. of Mechanical Engineering, University of Birjand, Iran,
e-mail: khkhalili@yahoo.com

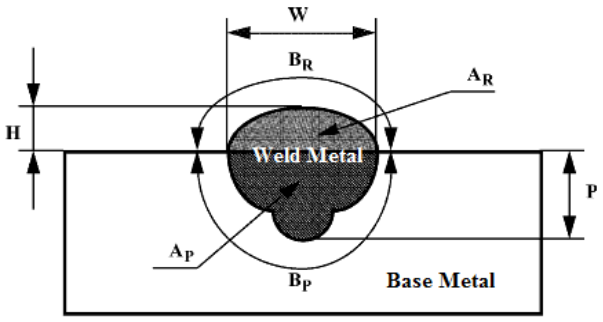

Fig. 1: Schematic cross-section of a welded plate and the weld bead geometry.

In recent years, a great deal of research has been carried out in the field of prediction and optimization of various welding processes to reach the desired weld bead geometry. For example, Dutta and Kumar carried out modeling of TIG welding using regression analysis and predicted the width and height of weld bead and back-side bead by means of their model [4]. Nagesh and Datta investigated the use of neural networks in predicting width and height of weld bead and back-side bead in TIG welding process [5]. Balasubramanian *et. al.* performed modeling of laser beam welding based on neural networks, and presented a model which was capable of predicting depth of penetration and weld bead width [6]. Sathiya *et. al.* carried out the modeling of laser beam welding by means of neural networks, and optimized its parameters by genetic algorithm [7]. The general implementation method of all these researches includes:

a) Carrying out welding process in experimental conditions.

b) Off-line Measurement of weld bead geometry parameters.

c) Using the results of these measurements for modeling of the welding process and optimizing process variables.

Considering the wide range of research in the field of prediction and optimization of various welding processes, it is necessary to present an appropriate approach for off-line measurement of weld bead geometry.

Nowadays, the need for cost reduction and quality improvement in the very competitive manufacturing industries has pushed the industry toward automating activities, in which great improvements has been done in the past few decades. With this regard, using machine vision systems as one of the automation tools is very effective in automatic inspection and measurement. Some of the important advantages of measurement by machine vision systems include: a) accurate measurement tools and their maintaining is not required, b) the system is non-contact and non-destructive, and, c) measurement is conducted with high speed and lower costs [8]. These advantages along with the ease of automation and integration have caused machine vision to replace conventional measurement methods in various research and industrial fields.

Existing problems in conventional measurement of weld bead geometry parameters by conventional measurement tools (such as calipers) has led to use of machine vision systems for measurement of these parameters. These problems include the need for skilled operators and spending too much time for accurate measurement, and also the absence of a suitable method for measuring the bead convexity length, the length of bead penetration boundary and bead total area. Moreover, manual tools such as calipers cannot be used to accurately measure the depth of penetration and height of weld bead. Some efforts have been made so far for off-line measurement of weld bead geometry by non-conventional methods. For example, Trang and Yang [9] measured weld profile by planimeter. Bowman and Quinn [10] and also Mashiri et. al. [11] used profile projector to measurement of weld bead geometry. These methods are not fully automated and furthermore, it is not possible to use them for measuring all weld bead geometry parameters. Also, such techniques are inherently inaccurate due to human errors. In this paper, a machine vision system is used to facilitate and to speed up the accurate measurement of weld bead geometry. This technique is performed on submerged arc welding of API X65 thermo-mechanical steel plates. Such steels have extensive use in large-diameter, long distance pipeline networks for natural gas transportation.

2. Submerged arc welding of the test plates

In this research, SAW was carried out on 50 steel plates of grade API X65 under different welding conditions. To do so, steel plates with a width of 100mm, length of 200 mm and thickness of 14.30 mm were provided. The welding current (I), voltage (V) and speed (S) of welding were considered as process variables in all experiments. Other effective parameters in submerged arc welding were been fixed during all the experiments. The experimental conditions used in these experiments are listed in Table.1. The welding equipment used in this research and some of the welded plates are shown in figs. 2 and 3, respectively.

Table 1

Experimental conditions used in Submerged arc welding of test plates

Elements	Types
Plate	API X65 Steel
Electrode	(AWS A 5.23 , EN 756, EN 12070) S2MO (3.2 mm Diameter)
Flux	(AWS(A 5.17 & A 5.23) , DIN 32522 & DIN EN 760) AMA OP 139

Fig. 2. welding equipment used in this research

Fig. 3. Some of the welded plates

3. Weld metal revelation in the cross section of plates

For measuring weld bead geometry parameters, it is necessary to cut the plates after welding process, as demonstrated in Fig.4. After cutting the plates, their cross sections were polished first. To reveal the weld metal in the cross section, the use a proper solution for etching is required.

Fig. 4: Cross section of a API X65 plate after welding.

During etching process, corrosion changes the color of weld metal in comparison with the base metal. Therefore, the selected solution must carry out the corrosion process in such a way that causes maximum visible contrast between weld metal and base metal regions. Higher contrast between the colors of these two regions reduces the next image processing operations and increases the accuracy of measurements. Therefore, to reach the best solution for etching the cross section of the plates, six acidic solutions were prepared and their results are investigated. These solutions include:

a) Nital solution:

This solution is widely used in etching steels. To produce Nital solution, a solution must be provided with 1-5% of nitric acid and 95-99% of ethyl alcohol

[12]. Thus, five Nital solutions with different nitric acid concentration (1%- 5%) were prepared.

b) Picral solution:

A proper Picral solution for etching steel contains 4% picric acid and 96% ethyl alcohol [25].

c) Picral+ Nital solution:

By combining Picral solution (4% picric acid dissolved in 96% ethyl alcohol) and Nital solution (2% nitric acid dissolved in 98% ethyl alcohol), an appropriate solution would be prepared for etching steel [12].

d) Diluted acid solution:

Hydrochloric acid, sulphuric acid and nitric acid are three known acids with strong acidity which cause corrosion in the surface of metals. These acids are rapidly dissolved in the water and could be diluted easily. For preparing water-acid solutions with various densities, each of the mentioned acids have been dissolved in 10 different quantities (1, 2,…10 units) with 100 units of distilled water. So, 30 different water-acid solutions are prepared for etching the cross section of plates. By carrying out some experiments, it was found that the mentioned acid solutions with a concentration less than 1 acid unit in 100 units of water had not a significant effect on the cross section of plates. Also, solutions with a concentration more than 10 acid units in 100 units of water, equally change the color of both weld metal and base metal regions and if they are used, these two regions could not be well separated.

Etching times for Nital, Picral and Nital+Picral solutions are considered 20 sec. [12]. Also the optimum times for etching by water-acid solutions are 18 min which were obtained from different experiments. After etching the plates by solutions, the average gray levels of base metal and weld metal pixels are measured in the images of their cross sections. In the next step, the difference between these two averages in each image was calculated (see Table 2). The criterion considered for evaluating various solutions is the difference between these two average gray levels. Considering the results, the sulphuric acid solution could be presented as a proper solution for etching the cross section of plates. This solution with a concentration of 4 acid units in 100 water units, had the best performance in separating the weld metal and base metal regions.

After the determination of the proper solution, the cross sections of all plates were etched in sulphuric acid solution. For evaluating the performance of the machine vision system in measurement of the depth of penetration, weld bead width and height, these parameters were measured by spending too much time and employing a skilled operator (by a caliper with 0.05 mm precision).

Table 2

Difference values between mean of gray-levels of base and weld metal pixels from etching by different solutions

No.	Solution	Difference of Gray-Levels between Weld Metal and Base Metal Pixels
1	HCL (7 units)+ H_20 (100 units)	8
2	H_2SO_4 (4 units)+ H_20 (100 units)	43
3	HNO_3 (9 units)+ H_20 (100 units)	21
4	Nital (%4)	15
5	Picral	6
6	Nital+Picral	7

4. Image acquisition

One of the key parameters in success of machine vision in tasks such as inspection it provide the camera with a well illuminated and well-arranged scene. Indeed, desired image removes most of the complexities in the next image processing steps. In this research, a standard flatbed scanner was used for image capturing of the cross section of the plates. Using this scanner eased most of the technical problems in preparing desired images from the cross section of the plates. Removing perspective, the fixed distance between the scanner lens and the cross section of plates, optimal lighting (in this case) and low cost were some of the most important advantages of using a scanner in this study.

5. Image processing

The first step in processing the initial image was to convert the RGB image into a HSV image with 256 gray levels. Fig. 5 shows the initial image of a plate's cross section, respectively. In the next step, the enhancement of base metal region in the image would be the objective of the processing. To reach this goal, the values of contrast and brightness were set to 78, 128 and respectively. These adjusted values were fixed during processing of all images. Also, the Median filter was used to remove the possible noise in the image, as shown in Fig. 6.

Fig. 5. Initial image of plate's cross section

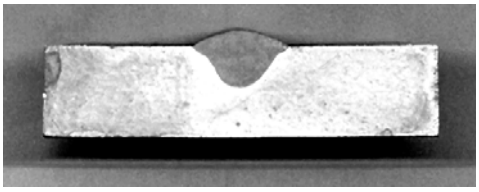

Fig. 6. The plate's cross section image after applying the Median filter.

Image enhancement makes suitable conditions for proper image segmentation. In this research, manual thresholding was used for image segmentation. To separate base metal from other regions in the image, the threshold level was chosen to be fixed at 180. After that, the thresholding was applied and the image was converted into a binary image. Then, the undesired regions in the binary image were removed (only the base metal was remained by advanced morphology and removing regions with small area), see Fig. 7.

Fig. 7. Separating base metal from other regions of the image

By the use of the initial image, the necessary image processing was applied for separating the plate's cross section from image background. After converting the RGB image into a HSL image with 256 gray levels, the contrast, brightness and were set to fixed values of 45, 128 respectively. These values caused better segmentation of plate's cross section from background. By applying manual thresholding and choosing the threshold level of 206, the plate's cross section was separated from image background. Again, the advanced morphology and removing regions with small area in the image was used to remove the undesired regions (resulted from image thresholding). Fig. 8 shows the binary image of plate's cross section which is separated from image background.

Fig. 8. separating the plate's cross section from image background.

By subtracting the resulted images 7 and 8 and using appropriate filters for removing undesired regions, weld metal was separated from other regions. The operations which were done by these filters include removing small regions, removing image boundary regions and limiting the first pixel of the region of interest in the directions X and Y of image. Fig. 9 shows the resulted image from subtraction of images shown in Fig. 7 and Fig. 8. Also, the resulted image from using various filters is shown in Fig. 10.

Fig.9. Separation of weld metal from other regions of image.

Fig. 10. Removing undesired regions of image by using various filters.

5.1. Measurement of weld bead geometry

By separating weld metal from other regions of image, suitable conditions were provided to automatic measurement of weld bead geometry parameters. Because all of the settings were the same as in measurements of weld bead geometry, calibration was summarized to determining the dimensional magnification ratio of images. Since the thickness of plate was a known value in its cross section image, it was used as a reference value. By measuring the plate thickness from its cross section image, the dimensional magnification ratio of each image was calculated automatically.

6. Results and discussion

As mentioned earlier, the sulphuric acid solution with the concentration of 4 units of acid in 100 units of water caused maximum difference (42 gray levels) between gray levels of weld metal and base metal pixels considering (see Table. 2). Fig. 11 shows the diagram of the average gray levels of weld metal and base metal pixels in 50 plates etched by this solution. Considering Fig. 11, the difference created between the average gray levels of weld metal and base metal pixels resulted in obtaining proper images of cross section of API X65 steel plates and it also made it possible to separate weld metal region from base metal region with minimum image processing.

The proposed procedure in this research was used to measurement of weld bead geometry parameters in submerged arc welding of API X65 steel plates. The obtained results from automatic measurement of penetration depth, weld bead width and height by using proposed vision system are presented in Table 3. For evaluating the performance of proposed method, the percentage error of machine vision measurements of penetration depth, weld bead width and height in comparison with measurements of these parameters by skilled operator was calculated and presented in Table 3. Other parameters of weld bead geometry were also measured by using the proposed vision system (see Table 4).

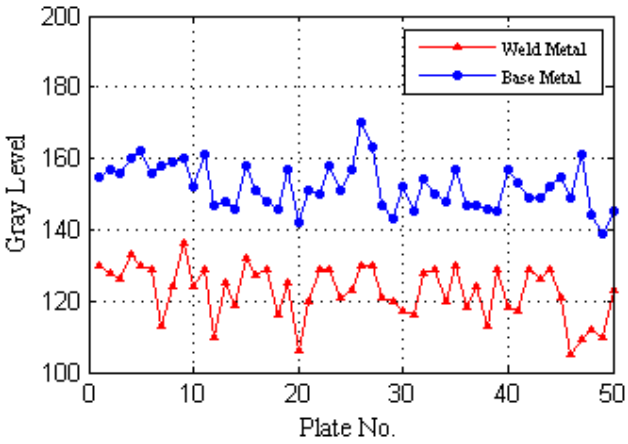

Fig. 11. The average gray levels of weld metal and base metal pixels in images of 50 plates etched by selected solution (4 units of sulphuric acid + 100 units of water)

Considering the experimental results in Table 3, it can be seen that the maximum difference in machine vision measurements in comparison with skilled operator measurements for depth of penetration, weld bead width and height parameters were 0.35mm, 1.44mm and 0.57mm respectively. Furthermore, the mean percentage errors of proposed vision system measurements of penetration depth, weld bead width and height were 2.31%, 1.6% and 4.74%, respectively. These percentage error values reveal the desired performance of proposed vision system for reliable measurement of weld bead geometry of submerged arc welded API X65 steel plates.

Table 3

Welding conditions and measurements of penetration depth (P), weld bead width (W) and height (H) from the proposed vision system.

Plate No.	Welding Conditions			Skilled operator measurements			Machine vision measurements			Percentage error of measurements (%)		
	Current (A)	Voltage (V)	Speed (cm/min)	P (mm)	W (mm)	H (mm)	P (mm)	W (mm)	H (mm)	P (%)	W (%)	H (%)
1	400	30	36	4.90	15.70	2.40	5.03	15.48	2.47	2.65	1.40	2.91
2	450	30	36	5.75	17.70	2.40	5.85	17.43	2.43	1.73	1.52	1.25
3	500	30	36	6.00	20.00	2.45	6.00	20.02	2.44	0.00	0.10	0.40
4	550	30	36	7.80	21.10	3.20	7.78	21.06	3.59	0.25	0.19	12.18
5	600	30	36	9.30	18.30	3.85	9.14	18.10	2.85	1.72	1.10	25.97
6	400	32	36	4.75	17.35	2.60	4.73	17.42	2.59	0.42	0.40	0.38
7	450	32	36	6.90	17.40	2.35	6.78	17.12	2.36	1.73	1.60	0.42
8	500	32	36	5.50	17.30	2.90	5.32	17.74	2.42	3.27	2.54	16.55
9	550	32	36	8.40	18.50	3.15	8.44	18.69	3.21	0.47	1.02	1.90
10	600	32	36	9.15	20.30	3.70	8.91	20.25	3.58	2.62	0.24	3.24
11	400	34	36	4.70	16.00	2.70	4.58	16.04	2.62	2.55	0.25	2.96
12	450	34	36	6.65	19.45	2.90	6.65	19.43	2.95	0.00	0.10	1.72

13	500	34	36	5.25	18.45	2.20	5.15	18.67	2.20	1.90	1.19	0.00
14	550	34	36	8.35	19.70	2.35	8.24	18.26	2.25	1.33	7.30	4.25
15	600	34	36	8.20	22.55	2.50	8.17	22.72	2.44	0.36	0.75	2.40
16	400	36	36	5.10	16.30	2.50	5.07	15.71	2.42	0.58	3.61	3.20
17	450	36	36	5.10	19.00	2.55	5.02	19.05	2.72	1.56	0.26	6.66
18	500	36	36	6.80	19.60	3.25	6.76	19.77	3.33	0.58	0.86	2.46
19	550	36	36	7.00	22.65	3.45	7.08	22.92	3.50	1.14	1.19	1.44
20	600	36	36	7.85	23.25	2.65	7.78	23.40	2.86	0.89	0.64	7.92
21	400	30	46	3.60	12.50	2.10	3.84	12.81	1.94	6.66	2.48	7.61
22	450	30	46	5.10	12.45	2.20	4.77	11.43	2.12	6.47	8.19	3.63
23	500	30	46	5.60	13.90	2.30	5.60	13.51	2.44	0.00	2.80	6.08
24	550	30	46	5.90	13.10	2.00	6.24	13.00	2.18	5.76	0.76	9.00
25	600	30	46	7.20	13.20	2.40	7.18	12.74	2.16	0.27	3.48	10.00
26	400	32	46	3.30	10.10	2.40	3.47	10.41	2.34	5.15	3.06	2.50
27	450	32	46	4.55	12.30	2.40	4.56	11.91	2.42	0.21	3.17	0.83
28	500	32	46	5.20	12.70	2.10	5.07	12.68	2.17	2.50	0.15	3.33
29	550	32	46	6.00	12.30	2.20	5.75	12.13	2.29	4.16	1.38	4.09
30	600	32	46	6.80	14.00	2.50	7.06	14.24	2.49	3.82	1.71	0.40
31	400	34	46	5.05	10.80	2.20	4.70	10.04	1.88	6.93	7.03	14.54
32	450	34	46	4.60	11.90	2.25	4.90	12.11	2.08	6.52	1.84	7.55
33	500	34	46	6.00	14.05	2.50	6.13	14.18	2.70	2.16	0.92	8.00
34	550	34	46	7.50	15.00	2.70	7.51	14.91	2.43	0.13	0.60	10.00
35	600	34	46	7.30	13.75	2.45	7.29	13.59	2.40	0.13	1.16	2.04
36	400	36	46	5.00	11.35	2.10	4.73	11.36	2.18	5.40	0.08	3.80
37	450	36	46	5.60	13.00	2.60	5.73	13.12	2.56	2.32	0.92	1.53
38	500	36	46	6.35	14.55	2.40	6.40	14.26	2.47	0.78	1.99	2.91
39	550	36	46	6.50	14.30	2.50	6.69	14.42	2.33	2.92	0.83	6.80
40	600	36	46	7.30	14.70	2.90	7.36	14.48	2.81	0.82	1.49	3.10
41	400	30	49	4.25	12.70	2.40	3.95	12.37	2.44	7.05	2.59	1.66
42	450	30	49	5.70	15.70	2.30	5.49	15.32	2.19	3.68	2.42	5.21
43	500	30	49	6.60	16.00	2.80	6.64	16.22	2.95	0.60	1.37	5.35
44	550	30	49	7.05	18.00	2.65	7.18	17.84	2.71	1.84	0.88	2.26
45	600	30	49	8.60	17.45	3.10	8.78	17.44	3.07	2.09	0.05	0.96
46	400	32	49	5.40	13.60	2.50	5.35	13.52	2.31	0.92	0.58	7.60
47	450	32	49	6.10	14.90	3.15	5.93	15.06	3.27	2.78	1.07	3.80
48	500	32	49	7.10	15.50	3.15	6.88	15.54	3.33	3.09	0.25	5.71
49	550	32	49	6.90	17.10	2.75	7.00	17.13	2.66	1.44	0.17	3.27
50	600	32	49	8.20	18.55	3.30	8.47	18.49	3.15	3.29	0.32	4.54

Table 4

Weld bead total area, bead reinforcement and bead penetration areas, length of bead penetration and bead reinforcement boundaries from the proposed vision system.

Plate No.	Bead Total Area (mm^2)	Bead Reinforcement Area (mm^2)	Bead Penetration Area (mm^2)	Length of Bead Penetration Boundary (mm)	Length of Bead Reinforcement Boundary (mm)
1	71.67	23.15	48.52	26.12	20.29
2	83.29	30.63	52.65	29.16	22.82
3	95.00	29.87	65.12	32.68	25.56
4	124.27	41.51	82.75	36.81	29.42
5	125.21	33.90	91.30	37.17	25.12
6	74.57	31.11	43.46	26.98	23.14
7	89.43	28.09	61.33	30.65	23.24
8	80.54	27.26	53.28	28.18	22.62
9	127.70	38.25	89.45	35.90	24.66
10	141.66	43.28	98.38	38.40	26.95
11	70.97	25.80	45.17	24.84	21.38

12	106.93	36.05	70.87	32.72	24.10
13	80.83	25.92	54.90	28.82	22.67
14	126.54	34.37	92.16	37.23	25.29
15	138.98	42.63	96.34	39.56	27.77
16	73.26	22.45	50.81	26.97	19.70
17	86.25	30.96	55.29	29.78	23.88
18	113.91	37.84	76.07	33.61	26.99
19	128.15	45.20	82.94	38.05	29.85
20	134.14	40.19	93.95	38.90	28.82
21	44.72	14.33	30.38	19.61	17.60
22	56.15	16.74	39.40	23.25	16.42
23	66.08	21.93	44.15	25.29	18.30
24	70.57	20.21	50.35	25.29	17.41
25	72.48	19.09	53.37	26.76	17.21
26	45.05	15.91	29.14	19.28	15.27
27	52.72	15.65	37.16	21.61	16.30
28	58.60	16.96	41.63	23.93	16.80
29	69.80	17.16	52.63	25.94	17.12
30	83.30	24.09	59.21	27.99	18.91
31	47.73	13.99	33.74	19.60	14.70
32	54.19	13.98	40.21	22.41	15.75
33	75.59	21.11	54.47	26.77	18.23
34	88.05	24.78	63.26	29.75	19.83
35	79.23	20.86	58.37	28.36	18.07
36	51.22	15.37	35.85	21.23	15.63
37	67.03	21.43	45.60	25.16	18.04
38	77.08	21.54	55.53	27.72	18.77
39	80.92	23.56	57.36	28.25	19.51
40	90.66	23.83	66.82	30.08	19.41
41	49.14	17.56	31.57	21.62	17.17
42	72.89	23.93	48.95	26.40	19.55
43	88.18	28.08	60.09	29.67	21.52
44	99.80	30.36	69.44	32.24	23.54
45	122.30	37.44	84.85	35.31	23.88
46	59.95	17.10	42.84	24.05	18.45
47	81.24	28.92	52.49	27.13	20.76
48	96.28	31.11	65.17	29.90	21.53
49	93.59	30.98	62.20	31.15	22.60
50	121.01	37.64	83.36	35.27	25.12

7. Conclusion

A machine vision system was proposed for off-line measurement of weld bead geometry in submerged arc welding of API X65 steel. For different values of welding voltage, current and speed, practical experiments were carried out on fifty API X65 steel plates by an automatic submerged arc welding machine. The test plates then were cut and their cross sections were polished. Next, the proper solution for etching the cross sections of plates for better revelation of the weld metal region was identified through extensive experimental work. The diluted sulphuric acid solution (4 acid units in 100 water units) generated the maximum difference between gray levels of weld metal and base metal regions. Finally, different images were taken from the etched cross section of plates and processed. The aim of image processing was to separate the weld metal from other regions in

order to measure the weld bead geometry parameters. The results showed that the proposed vision system had a desired performance in off-line measurement of weld bead geometry in submerged arc welding process of API X65 steel plates. Therefore, the proposed vision system could be used in off-line measurement of weld bead geometry in submerged arc welding of this grade of steel. The measured values could be used in training and testing stages of submerged arc welding modeling in order to reach the desired weld bead geometry in an industrial scale.

Acknowledgement

The supply of API X65 pipeline steel and the help on welding experiments by Sadid Pipe and Equipment Company (IRAN) is greatly acknowledged.

R E F E R E N C E S

[1] *K. Shinagawa and S. Ku*, Weld Imperfections and Preventive Measures, Kobe steel- LTD, Fourth edition, 2011.

[2] *U. Esme, M. Bayramoglu, Y. Kazancoglu and S. Ozgun,*"Optimization of weld bead geometry in TIG welding process using gray relation analysis and taguchi method", Materials and Technology, **vol. 43**, 2009, pp. 143-149

[3] *I.S. Kim, J.S. Son, S.H. Lee and P. Yarlagadda,*"Optimal design of neural networks for control in robotic arc welding", International Journal of Robotics and Computer Integrated Manufacturing, **vol. 20**, 2005, pp. 57-63

[4] *P. Dutta and D.K. Pratihar,*"Modeling of TIG welding process using conventional regression analysis and neural network-based approaches", Journal of Materials Processing Technology, **vol. 184**, 2007, pp. 56-68

[5] *D.S. Nagesh and G.L. Datta,*"Genetic algorithm for optimization of welding variables for height to width ratio and application of ANN for prediction of bead geometry for TIG welding process", Applied Soft Computing, **vol. 10**, 2010, pp. 897-907

[6] *K.R. Balasubramanian, G. Buvanashekaran and K. Sankaranarayanasamy,*"Modeling of laser beam welding of stainless steel sheet butt joint using neural networks", Journal of Manufacturing Science and Technology, **vol. 3**, 2010, pp. 80-84

[7] *P. Sathiya, K. Panneerselvam and M.Y. Jaleel,*"Optimization of laser welding process parameters for super austenitic stainless steel using artificial neural networks and genetic algorithm", Materials and Design, **vol. 36**, 2012, pp. 490-498

[8] *E.N. Malamas, G.M. Petrakis, M. Zervakis, L. Petit and J. Legat,*"A survey on industrial vision systems, applications and tools", Image and Vision Computing, **vol. 21**, 2003, pp. 171-188

[9] *Y.S. Tarng and W.H. Yang,*"Optimisation of the weld bead geometry in gas tungsten arc welding by the Taguchi method", International Journal of Adv. Manuf. Technol., **vol. 14**, 1998, pp. 549-554

[10] *M.D. Bowman and B.P. Quinn,*"Fillet weld profile measurements", Experimental Techniques, **vol. 5**, 1995, pp. 21-24

[11] *F.R. Mashiri, X.L. Zhao and P. Grundy,*"Effects of weld profile and undercut on fatigue crack propagation life of thin-walled cruciform joint", Thin-Walled Structures, **vol. 39**, 2001, pp. 261-285

[12] *A.O. Benscoter and B.L. Bramfitt,* Metallography and Microstructures of Low-Carbon and Coated Steels, ASM Hand Book, ASM International, vol. 9, 2004.